Biophysical Chemistry 42 (1992) 101–109
Elsevier Science Publishers B.V., Amsterdam

BIOCHE 01619

The binding of 4′,6-diamidino-2-phenylindole to bovine serum albumin

Alberto Mazzini [a,*], Paolo Cavatorta [a], Monica Iori [a], Roberto Favilla [a] and Giorgio Sartor [b]

[a] *Division of Biophysics and Molecular Biology, Department of Physics, and* [b] *Institute of Biological Chemistry, University of Parma, 43100 Parma (Italy)*

(Received 25 February 1991; accepted in revised form 12 June 1991)

Abstract

The binding of 4′,6-diamidino-2-phenylindole (DAPI) to bovine serum albumin (BSA) has been investigated between pH 6 and 8, in 0.05 *M* phosphate buffer at 20 °C, by fluorescence titrations and the results analyzed according to a procedure previously reported (R. Favilla and A. Mazzini, Biochim. Biophys. Acta 788 (1984) 48). The dye binds to the protein with a blue shift of about 4 nm in its fluorescence emission maximum, but with an enhancement factor of 10 of its fluorescence quantum yield. The dissociation constant decreases from 100 μM to 54 μM as the pH is increased from 6 to 8, with a constant number of nearly three equivalent binding sites. The complete displacement of DAPI bound to BSA by Ca^{2+} suggests a possible specificity of this substantially electrostatic interaction. The fluorescence decay of DAPI bound to the protein shows a double exponential kinetics, with a $\tau_1 = 0.97$ ns and $\tau_2 = 2.78$ ns. These results, compared with those obtained for DAPI alone, $\tau_1 = 0.16$ ns and $\tau_2 = 2.8$ ns, are rationalized in terms of two different rotamers of DAPI. Both rotamers are able to bind to the protein, but only one of them undergoes an intramolecular proton transfer, from the 6-amidinium group to the indole aromatic ring, in the excited singlet state of DAPI alone. When DAPI interacts with BSA this transfer does not occur and consequently a large increase of fluorescence is observed. The fluorescence anisotropy decay of DAPI bound to BSA can be analyzed in term of a single exponential with a correlation time of 34 ns. Preliminary experiments with other acidic proteins suggest that DAPI can be used as an useful probe for negatively charged proteins or domains.

Keywords: 4′,6-Diamidino-2-phenylindole (DAPI); Fluorescence lifetime and anisotropy; Bovine serum albumin (BSA); Binding

1. Introduction

The fluorescent dye DAPI (4′,6-diamidino-2-phenylindole) binds to double stranded deoxyribonucleic acids with a large enhancement of its fluorescence quantum yield [1]. Since its optical emission, absorption and circular dichroism spectra are modified upon binding, this molecule has been extensively used for spectroscopic studies on nucleic acids [2–4] and for biochemical cytological analysis [5–7].

Several investigations on polydeoxynucleotides of different base sequence [8,9] have indicated that DAPI preferably binds to AT clusters, but not to single stranded DNA. Although the binding mechanism has not been fully elucidated, two

* To whom correspondence should be addressed.

kinds of interaction between the dye and DNA have been suggested: electrostatic bonds, between the polynucleotide backbone phosphate groups and the amidine positive groups of the dye, and hydrogen bonds, between acceptor groups on close AT base pairs in the narrow groove (namely O-2 of thymidine and N-3 of adenine) and amidine donor groups on DAPI [10].

However, the large use of DAPI in staining procedures of chromosomes as well as of whole cell raises the problem of its specificity towards nucleic acids with respect to other cellular components.

In preliminary experiments, we observed that the fluorescence of DAPI increased upon addition of either lipid vesicles or proteins. These results, while suggesting a careful use of DAPI in cytological studies, have stimulated us to investigate the interactions of this dye with molecules other than nucleic acids more deeply.

In this first work we report on the interaction between DAPI and bovine serum albumin (BSA) as assayed through fluorescence titrations and measurements of both static and dynamic anisotropy, whereas the interaction of DAPI with lipid vesicles will be dealt with in a next paper. The observed effects of salts as well as the dependence of the dissociation constant on pH indicate the essentially electrostatic nature of the interaction. The interaction of DAPI with BSA has been further characterized by time resolved fluorescence decay and anisotropy measurements. From experiments with other proteins DAPI turned out to be able to bind only to negatively charged proteins, thus raising the possibility of using it as a probe for acidic proteins and/or negatively charged domains on the protein surface.

2. Materials and methods

4′,6-Diamidino-2-phenylindole (DAPI) and fatty acid free bovine serum albumin (BSA) were purchased from Sigma Chemical Co. and used without further purification. Buffer solutions were prepared by dissolving Merck salts in water purified through a Milli-RO plus Milli-Q system (Millipore Corp., USA). Fluorescence titrations were carried out at pH 6, 7 and 8 (0.05 M sodium phosphate buffer) and 20 °C using a Jasco model FP 770 spectrophotofluorimeter equipped with a thermostatically controlled cell holder.

Two sets of titration experiments were performed by monitoring the fluorescence of DAPI, according to the progressive dilution method: at variable BSA and constant DAPI concentration (type I titration; $\lambda_{ex} = 380$ nm; $\lambda_{em} = 455$ nm), and viceversa (type II titration; $\lambda_{ex} = 400$ nm, $\lambda_{em} = 455$ nm). In this case a longer excitation wavelength was chosen in order to minimize inner filter effects due to DAPI.

The concentration of DAPI was calculated from its UV spectrum using an $\varepsilon_{344} = 23030\ M^{-1}\ cm^{-1}$ [11]. For absorbances higher than 0.1, corrections for inner filter effect were made by means of a calibration curve of the fluorescence intensity vs. [DAPI]. A correction factor higher than 1 was applied for type II titrations, when the concentration of DAPI exceeded 250 μM.

The binding constants k_d and the number of binding sites n have been evaluated according to a previously published paper [12].

Static fluorescent anisotropy experiments were carried out using two Polaroid polarizers HPN'B mounted on excitation and emission beams and the fluorescence anisotropy was evaluated according to the following relationship:

$$A = \frac{I_{vv} - I_{vh}G}{I_{vv} + 2I_{vh}G}$$

where I is the fluorescence intensity, 'v' and 'h' refer to the vertical and horizontal orientation of the excitation and emission polarizers and the correction factor $G = I_{hv}/I_{hh}$ [13,14].

Fluorescence lifetimes were measured using a single photon counter fluorimeter. The light source was a pulsed nitrogen flash lamp (199F Edinburg Instruments) pulsed at 20 kHz and the stop photomultiplier was a Philips XP2020Q. Fast NIM electronics were from ORTEC, Tennelec and Silena.

Fluorescence decays of the dye in the different experimental conditions were acquired alternatively with lamp decays and summed until at least

10000 counts at the peak channel were collected. Data were analyzed by the method of non-linear least square analysis according to the global procedure of J.R. Knutson et al. [15] and the goodness of fit was judged from the χ^2 and from the randomness of the residuals. The time resolved fluorescence anisotropy was measured by monitoring the decay of the parallel (I_{vv}) and perpendicular (I_{vh}) components of the emitted light according to:

$$A(t) = \frac{I_{vv}(t) - I_{vh}(t)G}{I_{vv}(t) + 2I_{vh}(t)G}$$

Anisotropy decay, $A(t)$, and total intensity, $I(t)$, decay parameters were obtained from the fitting of the experimental data $I_{vv}(t)$ and $I_{vh}(t)$ according to:

$$I_{vv}(t) = \tfrac{1}{3}I(t)[1 + 2A(t)]$$

$$I_{vh}(t) = \tfrac{1}{3}I(t)[1 - A(t)]$$

using the global procedure [15]. In particular $I(t)$ and $A(t)$ were each assumed to be a sum of exponentials:

$$I(t) = \sum \alpha_i \, e^{-t/\tau_i}$$

$$A(t) = A_0 \sum \beta_i \, e^{-t/\Phi_i}$$

In the formulas A_0 is the anisotropy at time zero, Φ_i are the correlation times, τ_i are the fluorescence lifetimes, α_i and β_i are the pre-exponential factors.

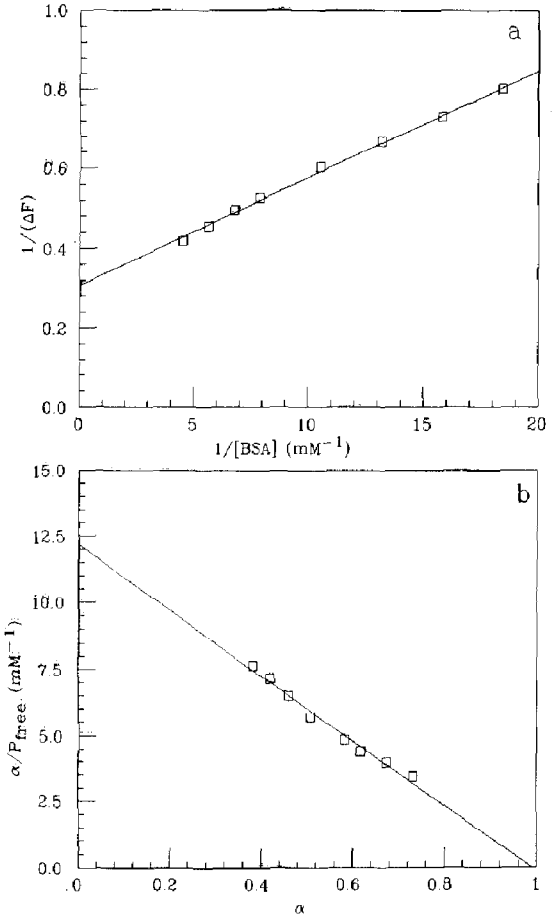

Fig. 1. Binding of DAPI to bovine serum albumin (BSA): Type I titration. (a) Double reciprocal plot, and (b) Scatchard-like plot. [DAPI] = 10 μM, [BSA] variable from 220 μM to 50 μM in phosphate buffer 0.05 M pH 7, $T = 20\,^{\circ}C$. The fluorescence intensity was measured at $\lambda_{em} = 455$ nm and $\lambda_{ex} = 380$ nm; $k_d = 81$ μM and $\Delta F^{I}_{max} = 3.26$. (see text for definition of α and ΔF^{I}_{max}).

3. Results

3.1 Titrations

3.1.1 Type I

Several fluorescence titrations at variable BSA (from 220 μM to 50 μM) and constant DAPI (10 μM) were carried out. By extrapolation of double reciprocal plots ($1/\Delta F$ versus $1/[BSA]$) at infinite protein concentration, a ΔF_{max} was obtained and called ΔF^{I}_{max} (Fig. 1a). This value represents the increase of fluorescence of 10 μM DAPI bound to the highest affinity sites.

We have then calculated the fraction of ligand bound as $\alpha = \Delta F/\Delta F^{I}_{max}$, the fluorescence enhancement factor of $DAPI_{bound}$ with respect to $DAPI_{free}$ as $Q = F_{max}/F_0$ and the dissociation constant k_d of the first binding site (81 μM) from the slope of the linear plot of $\alpha/[BSA]_{free}$ versus α (Scatchard-like plot) (Fig. 1b and Table 1).

3.1.2 Type II

In this case BSA was kept constant (10 μM) and the ligand was varied from 75 μM to 260 μM. A new ΔF_{max} (ΔF^{II}_{max}) was obtained from the

Table 1

Values of k_d, n and ratio of quantum yields (Φ) of DAPI bound and DAPI free, relative to the binding of DAPI to BSA at three different pHs

Parameter	pH		
	6	7	8
Φ_{bound}/Φ_{free}	11.6	10.9	9.8
k_d	~100 μM	~95 μM	~54 μM
n	2.8	2.7	2.7

double reciprocal plot at infinite DAPI concentration (Fig. 2a). Accounting for the different concentrations of the limiting reagent ([DAPI]$_l$ in

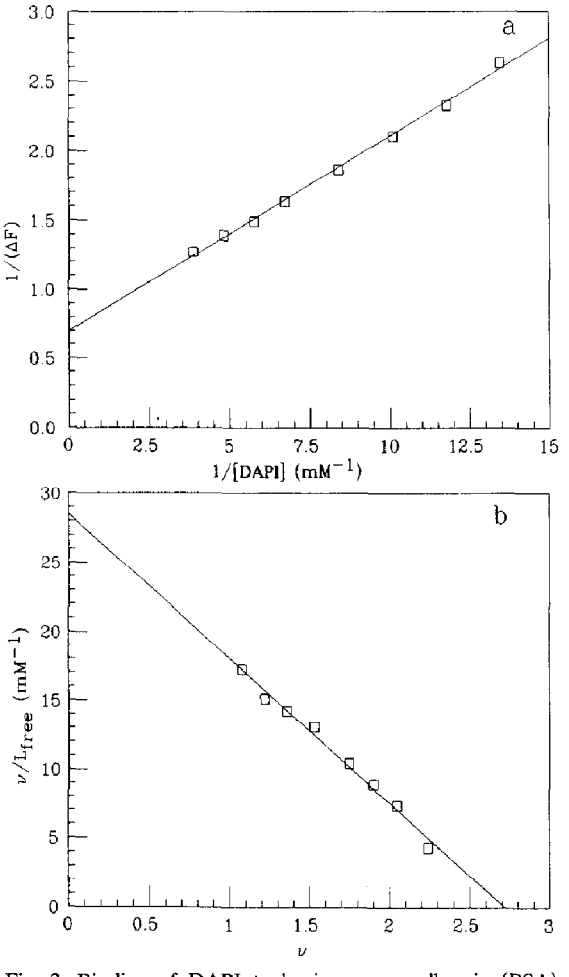

Fig. 2. Binding of DAPI to bovine serum albumin (BSA): Type II titration. (a) Double reciprocal plot, and (b) Scatchard plot. [DAPI] variable from 260 μM to 75 μM, [BSA] = 10 μM in phosphate buffer, 0.05 M pH 7, T = 20 °C, λ_{em} = 455 nm, λ_{ex} = 400 nm). k_d = 95 μM and ΔF^{II}_{max} = 1.42 (see text for definition of ν and ΔF^{II}_{max}).

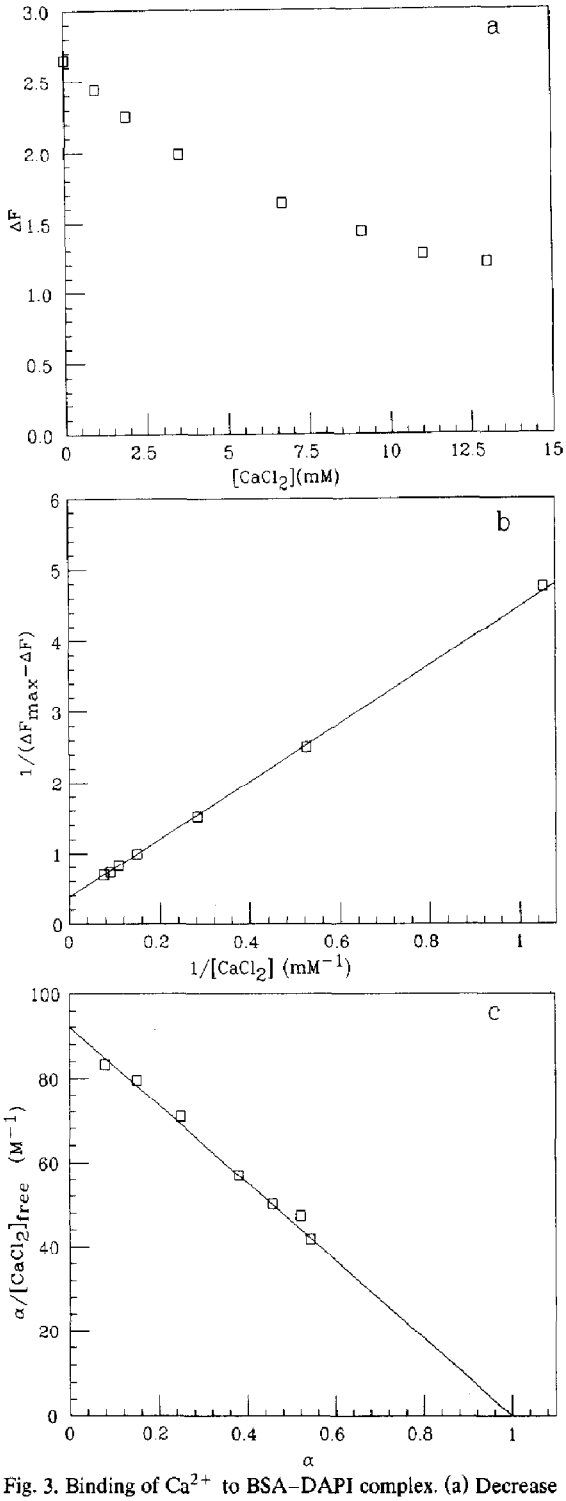

Fig. 3. Binding of Ca^{2+} to BSA–DAPI complex. (a) Decrease of fluorescence intensity of DAPI bound to BSA, (b) Double reciprocal plot, and (c) Scatchard-like plot. [DAPI] = 10.8 μM, [BSA] = 250 μM, [$CaCl_2$] variable from 0 to 12.5 mM in Tris-HCl buffer 0.05 M pH 7, T = 20 °C, λ_{em} = 455, λ_{ex} = 380 nm, k_d = 11.1 mM and ΔF_{max} = 2.62 (see text for definition of α).

type I and $[BSA]_{II}$ in type II titration) and the different absorbance of DAPI at the two different λ_{ex} used (Abs_{380} in type I and Abs_{400}, in type II titrations) a normalized ΔF^{I}_{max} ($\Delta F^{I'}_{max}$) can be calculated according to the following relation:

$$\Delta F^{I'}_{max} = \Delta F^{I}_{max} \frac{[BSA]_{II} Abs_{400}}{[DAPI]_{I} Abs_{380}}$$

The function of saturation $\nu = \Delta F / \Delta F^{I'}_{max}$ can then be used to draw a Scatchard plot (Fig. 2b): the experimental points are well fitted by a straight line ($k_d = 95\ \mu M$) and extrapolate to a number of sites equal to 2.7, suggesting a simple binding mechanism of three identical or very similar independent sites.

The n-value was confirmed by comparing ΔF^{II}_{max} with $\Delta F^{I'}_{max}$ according to:

$$n = \frac{\Delta F^{II}_{max}}{\Delta F^{I'}_{max}}$$

3.1.3. Effect of salts

Fluorescence intensity measurements were performed on solutions of DAPI (10.8 μM) and nearly saturating BSA (250 μM) in the presence of salts at various concentrations, in order to evaluate the electrostatic contribution to the interaction between the dye and the protein. In particular, we observed that Ca^{2+} ions were able to markedly reduce the fluorescence intensity, suggesting a strong competition between Ca^{2+} ions and DAPI for the binding to the protein. In fact, the value of ΔF_{max} extrapolated from the double reciprocal plot of $1/\Delta F_{max}$ vs. $1/[CaCl_2]$, indicates that the fluorescence of DAPI at infinite salt concentration is equal to that of $DAPI_{free}$ (F_0) (Figs. 3a and b).

From the slope of the Scatchard-like plot (Fig. 3c) the dissociation constant of Ca^{2+} could be determined ($k_d = 11$ mM) assuming:

$$\alpha = \frac{[DAPI]_{bound}}{[DAPI]_{tot}} = \frac{\Delta F}{\Delta F_{max}}$$

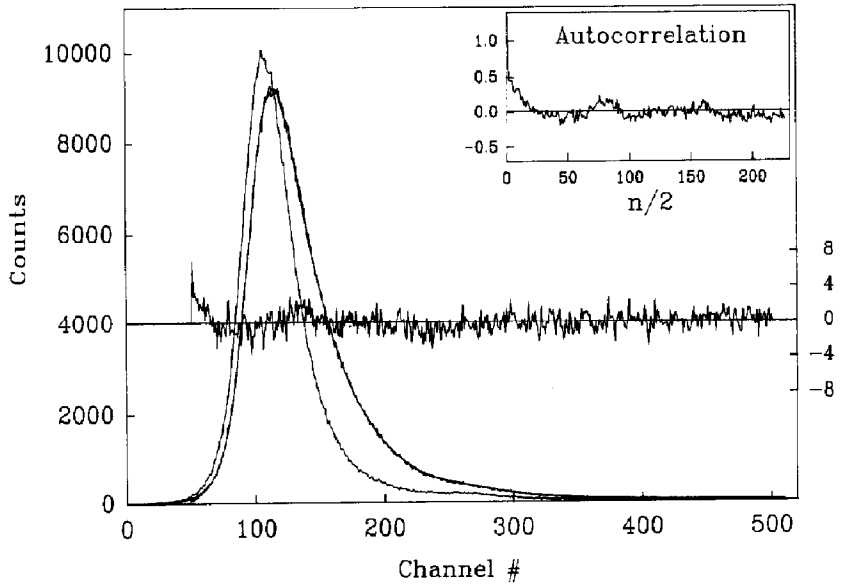

Fig. 4. Fluorescence decay profile of DAPI bound to BSA. The peak centered at about 9 ns (channel # 105) is the instrumental response function, the noisy plot is the decay of DAPI (10 μM) bound to BSA (280 μM) in phosphate buffer 0.05 M, pH 7, at $T = 20\,^{\circ}C$, $\lambda_{ex} = 350$ nm, $\lambda_{em} = 450$ nm, channel width = 0.086 ns, emission band pass 4 nm. The superimposed smooth line represents the convoluted fitted function and the mid graph is the plot of weighted residuals, whereas in the upper right corner the autocorrelation of the residuals is represented.

and

$$[Ca^{2+}]_{free} = [Ca^{2+}]_{tot} - \alpha[DAPI]_{tot} \simeq [Ca^{2+}]_{tot}$$

Preliminary experiments on BSA with other salts (NaCl and $CuCl_2$) also showed competition with DAPI, though not absolute (data not shown).

3.1.4 Decay associated spectra

A typical fluorescence decay of DAPI complexed with BSA is shown in Fig. 4. The deconvolution from the lamp profile gave a good χ^2 value (≤ 1.8) with a bi-exponential fit ($\tau_2 = 2.83$ ns and $\tau_1 = 0.97$ ns). The long component had a value very similar to that previously observed with DAPI alone ($\tau_2 = 2.78$ ns), whereas the short life time component had a larger value than that found for DAPI in buffer solution ($\tau_1 = 0.16$ ns). The decay associated spectra of DAPI alone and DAPI bound to BSA (Figs. 5a and 5b) showed two distinct emission components, one relative to the longer lifetime with a maximum wavelength near 390 nm, and the other substantially more towards the red, but quite different relative intensities in the two cases. The normalized pre-exponential factors α_i and the fractional fluorescences F_i at different wavelengths are shown in Tables 2(a) and 2(b) for DAPI bound and DAPI free, respectively.

3.2 Anisotropy measurements

3.2.1 Static fluorescence anisotropy

In order to better characterize the binding of DAPI to BSA and to verify the motional freedom of DAPI bound to BSA, measurements of static fluorescence anisotropy were carried out ($\lambda_{ex} =$ 350 nm and $\lambda_{em} = 450$ nm) on DAPI bound to BSA ($A = 0.283$) and compared to those on DAPI alone ($A = 0.107$). The large enhancement of A observed upon binding of DAPI to BSA was similar to that of DAPI bound to DNA ($A =$ 0.271), but still significantly smaller than that measured in viscous solvents at low temperature, e.g. propylene glycol ($A = 0.376$) [10].

3.2.2 Time resolved anisotropy

Figure 6 shows a typical anisotropy decay of DAPI bound to BSA. The anisotropy parameters

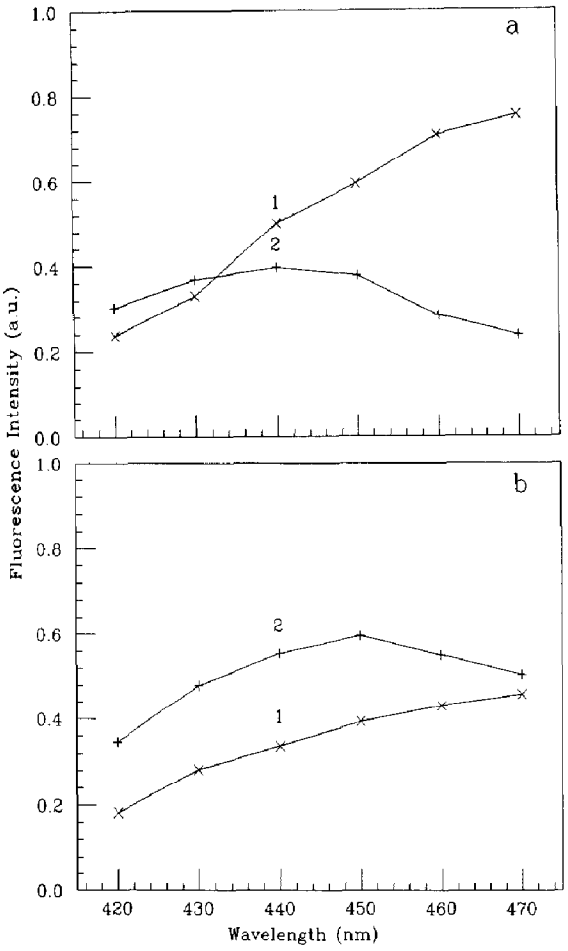

Fig. 5. Decay associated spectra. (a) Time resolved emission spectra of 10 μM DAPI alone in 0.05 M phosphate buffer, pH 7. (1) spectrum of 0.16 ns component; (2) spectrum of 2.78 ns component. (b) Time resolved emission spectra of DAPI bound to BSA in phosphate buffer pH 7, 0.05 M ([DAPI] = 10 μM and [BSA] = 280 μM). (1) spectrum of 0.97 ns component; (2) spectrum of 2.83 ns component.

Table 2(a)

Fluorescence decay parameters of DAPI (10 μM) in 0.05 M phosphate buffer, pH 7. α_1, F_1, α_2 and F_2 are normalized pre-exponential factors and fractional fluorescences relative to $\tau_1 = 0.16$ ns and $\tau_2 = 2.78$ ns, respectively

λ (nm)	F_2	α_2	F_1	α_1
420	0.508	0.057	0.492	0.943
430	0.524	0.061	0.476	0.939
440	0.441	0.045	0.559	0.955
450	0.386	0.036	0.614	0.964
460	0.281	0.023	0.719	0.977
470	0.240	0.018	0.760	0.982
480	0.219	0.016	0.781	0.983

Table 2(b)

Fluorescence decay parameters of DAPI bound to BSA in 0.05 M phosphate buffer, pH 7 ([BSA] = 280 μM; [DAPI] = 10 μM), α_1 and F_1, α_2 and F_2 are normalized pre-exponential factors and fractional fluorescences relative to $\tau_1 = 0.97$ ns and $\tau_2 = 2.83$ ns, respectively

λ (nm)	F_2	α_2	F_1	α_1
420	0.659	0.401	0.340	0.599
430	0.647	0.388	0.352	0.611
440	0.641	0.381	0.359	0.619
450	0.653	0.394	0.347	0.606
460	0.564	0.308	0.436	0.692
470	0.523	0.274	0.477	0.725
480	0.584	0.327	0.415	0.673

obtained from data analysis, as reported in Section 2, were $A_0 = 0.301$ and $\Phi = 34 \pm 2$ ns. This correlation time is in fairly good agreement with the correlation time ($\simeq 29$ ns) obtained for a spherical molecule from the Stokes–Einstein equation:

$$\Phi = V_h \eta / kT$$

where V_h denotes the hydration volume of BSA (cm^3); η is the viscosity of the solvent (Poise); k is Boltzmann's constant (erg K^{-1}); T the absolute temperature (K). Although BSA is assumed to be a spherical molecule, the volume V_h is calculated considering a prolate ellipsoid of revolution with major and minor axes of 140 Å and 40 Å respectively [16] including an hydration factor of 2.4 [17].

4. Discussion

To date DAPI has been utilized only as a probe for nucleic acids and fluorimetric studies in this perspective clearly show that, when bound to DNA, it increases its quantum yield of a factor near 20 [2,10]. However, our measurements on solutions of DAPI in the presence of BSA together with preliminary experiments on negatively charged proteins (namely pepsin, human serum albumin, yeast alcohol dehydrogenase and hemocyanine, data not shown) revealed a large enhancement of fluorescence intensity of the dye

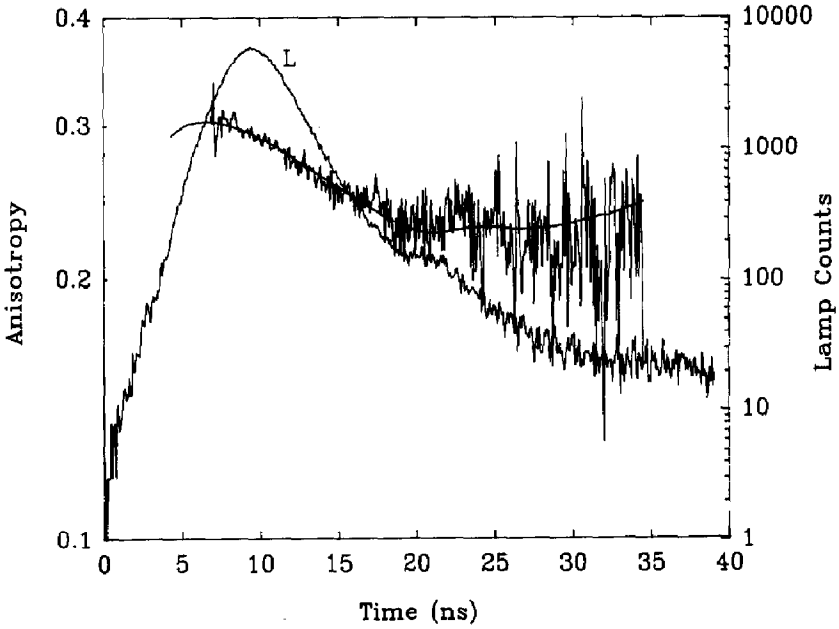

Fig. 6. Anisotropy decay. Reconstructed anisotropy decay from experimental data (noisy curve) and fitted anisotropy (smooth curve) from $A(t) = 0.301\ e^{-t/34}$ convoluted with the lamp function (L). Experimental conditions are the same as for Fig. 4.

complexed with these molecules, whereas no change of fluorescence intensity was observed with two positively charged proteins (lysozyme and ribonuclease, data not shown).

In this work we have characterized some fluorescence properties of DAPI–BSA complexes. The emission spectrum of DAPI bound to BSA showed a little shift of its maximum from 459 nm to 455 nm and the quantum yield increased of a factor 10 with respect to DAPI alone. Furthermore, from time resolved fluorescence analysis, two decay times were obtained both for DAPI alone ($\tau_1 = 0.16$ ns and $\tau_2 = 2.78$ ns) and bound to BSA ($\tau_1 = 0.97$ and $\tau_2 = 2.83$ ns). This behaviour is similar to that observed for DNA–DAPI complexes, where no change of the emission spectrum, a fluorescence enhancement factor of 20 and two fluorescence lifetimes ($\tau_1 = 3.85$ ns and $\tau_2 = 1.0$ ns) were observed [2]. In that work, DAPI was proposed to exist in two different conformations: one in which the indole ring is planar with the 6-amidine substituent (R1) and the other in which the substituent is rotated out of the indole plane (R2). In the planar conformer the indole ring becomes very basic in the excited single state (R1*) and a proton transfer from amidinium group to the indole ring can occur. The new species (RH1*) then decays with a short decay time of 0.14 ns and emission maximum near 490 nm. The lower basicity of the other conformer in the existed state (R2*) prevents the intramolecular proton transfer, therefore this fluorescent component shows a longer decay time (2.86 ns) and a maximum at 440 nm (see Scheme I).

Also the shape of decay associated spectra does not change substantially for DAPI alone and DAPI bound to BSA, moreover the lifetimes for the dye bound are quite similar to those obtained for DAPI alone at high pH values, where the proton transfer is absent [2].

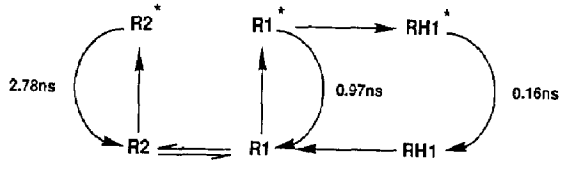

Scheme I

These results suggest that when DAPI binds to BSA, electrostatic interactions between the negative charges of the protein and the positive charges of the two amidinium groups prevent the intramolecular proton transfer from the 6-amidinium group in the excited singlet state of DAPI bound. The observed decay time of about 1 ns and the large fluorescence quantum yield enhancement can then be attributed to the excited singlet state of R1. The longer lifetime of DAPI bound (2.83 ns), quite similar to that observed with DAPI alone (2.78 ns), does not mean that the rotamer R2 is not involved into the binding, because the corresponding normalized pre-exponential term increases from 0.02 for DAPI alone to 0.3 for DAPI bound. Furthermore this behaviour provides evidence for a shift of the equilibrium between the 2 rotamers towards R2. The higher quantum yield of DAPI and the longer lifetime τ_1 (3.81 ns) of DAPI complexed to DNA with respect to the case of DAPI bound to BSA, can be explained assuming that the dye, bound in the minor groove of the double helix, is more shielded from the solvent than when bound to BSA.

The fluorescent anisotropy decay measurements ($A_0 = 0.301$ and correlation time $\Phi = 34$ ns) are in good agreement with the results reported for BSA in the literature [17]. Although the BSA has a shape of prolate ellipsoid and hence two correlation times should be expected for a fluorescence probe randomly distributed on the protein surface [18], the analysis of the anisotropy decay with a bi-exponential fit gave two correlation times of 58 ns and 3.88 ns with less satisfying statistical parameters. This is probably due to the intrinsic difficulty of determining a long correlation time (30–40 ns) by means of a short lifetime probe ($\simeq 2$ ns) [18].

The marked increase of fluorescence intensity associated with the binding of DAPI to BSA has been exploited by performing several titrations in a large concentration range. A Scatchard analysis of these titrations gave values of k_d near 90 μM and n near 3 at pH 7. Because k_d decreases from 100 to 54 μM going from pH 6 to pH 8, the

interaction between dye and BSA becomes tighter as the net negative charge of the macromolecule increases. The essentially electrostatic character of the interaction is also confirmed by the displacement of DAPI from BSA observed in the presence of calcium ions. The k_d value of 11 mM for the dissociation of Ca^{2+} from BSA, obtained from a Scatchard-like plot, is in good agreement with that measured with an ion specific electrode and relative to three equivalent sites [19]. Under our experimental conditions ([BSA] = 250 μM; [DAPI] = 10.8 μM), considering that DAPI is mainly bound to only one of the three independent sites on BSA, and that the dye is completely displaced by calcium ions, it is possible that the binding sites for DAPI and calcium are the same. The presence of other salts, such as NaCl and $CuCl_2$, strongly reduced the binding of DAPI to BSA, thus confirming a large electrostatic contribution to the interaction of DAPI with BSA.

The fact that DAPI binds to three binding sites may be rationalized with the presence of three structurally similar domains [16]. This result may be compared with others obtained with different ligands e.g. tryptophan and indole derivatives which bind to only two sites with similar dissociation constants [20], whereas the aromatic ligand 1-anilino-8-naphthalene sulfonate (ANS) binds to BSA to six equivalent sites [21].

Moreover a comparison of our results with those obtained for DAPI–DNA system shows that DAPI binds much more tightly to DNA (k_d values reported for DNA [1,22] are two to three orders of magnitude lower than those for BSA).

It may be worth mentioning that our preliminary experiments indicate DAPI is able to interact with phospholipid vesicles, thus suggesting also natural membranes as possible targets for this dye. Considering the multitude of potential targets (negatively charged proteins and membrane systems), we suggest DAPI to be used carefully as an *in vivo* probe.

In conclusion, we have demonstrated that DAPI binds to the negatively charged protein BSA through a substantially electrostatic mechanism. These results lay a fundation for the use of DAPI as fluorescent probe of structural and conformational aspects of negatively charged proteins or domains.

References

1 J. Kapuscinski and B. Skoczylas, Nucleic Acids Res. 5 (1978) 3775.
2 A.G. Szabo, D.T. Krajcarski, P. Cavatorta, L. Masotti and M.L. Barcellona, Photochem. Photobiol. 44 (1986) 143.
3 G. Manzini, M.L. Barcellona, M. Avitabile and F. Quadrifoglio, Nucleic Acids Res. 11 (1983) 8861.
4 J. Kapuscinski, J. Histochem. Cytochem. 38 (1990) 1323.
5 A.S. Waggoner, in: Flow cytometry and sorting, eds. R.M. Melamed, T. Lindmo and M.L. Mendelsohn, Fluorescent probes for cytometry (Wiley–Liss, New York, NY, 1990) p. 209.
6 Y.S. Fan, L.M. Davis and T.B. Shows, Proc. Natl. Acad. Sci. U.S.A. 87 (1990) 6223.
7 G. Bottiroli, A.C. Croce, G. Gerzeli and S. Barni, Cell Biophys. 15 (1989) 249.
8 J. Kapuscinski and W. Szer, Nucleic Acids Res. 6 (1979) 3775.
9 P. Cavatorta, L. Masotti and A.G. Szabo, Biophys. Chem. 22 (1985) 11.
10 M.L. Barcellona and E. Gratton, Eur. Biophys. J. 17 (1990) 315.
11 M. Avitabile, N. Ragusa, M.L. Barcellona and L. Masotti, Ital. J. Biochem. 31 (1985) 90.
12 R. Favilla and A. Mazzini, Biochim. Biophys. Acta 788 (1984) 48.
13 Y. Paoletti and J.P. Le Pecq, Anal. Biochem. 31 (1969) 33.
14 J. Azumi and S.P. Mc Glynn, J. Chem. Phys. 37 (1962) 2413.
15 J.R. Knutson, J.M. Beechem and L. Brand, Chem. Phys. Lett. 102 (1983) 501.
16 T. Peters Jr., Adv. Prot. Chem. 37 (1985) 161.
17 J. Yguerabide, F. Epstein and L. Stryer, J. Mol. Biol. 51 (1970) 573.
18 P. Wahl, in: Biochemical fluorescence: Concepts, vol. 2, eds. R.F. Chen and H. Edelhoch, (Marcel Dekker, New York, NY, 1975) p. 1.
19 N. Fogh-Andersen, Clin. Chem. 23 (1977) 2122.
20 N.P. Sollene, H.-L. Wu and G.E. Means, Arch. Biochem. Biophys. 207 (1981) 264.
21 D. Essassi, R. Zini and J.P. Tillement, J. Pharm. Sci. 79 (1989) 9.
22 M.L. Barcellona, R. Favilla, J. von Berger, M. Avitabile, N. Ragusa and L. Masotti, Arch. Biochem. Biophys. 250 (1986) 48.